

Increasing Plasma Membrane Phosphatidylinositol(4,5)Bisphosphate Biosynthesis Increases Phosphoinositide Metabolism in *Nicotiana tabacum*

Yang Ju Im,^a Imara Y. Perera,^a Irena Brglez,^a Amanda J. Davis,^a Jill Stevenson-Paulik,^{b,1} Brian Q. Phillippy,^a Eva Johannes,^a Nina S. Allen,^a and Wendy F. Boss^{a,2}

^aDepartment of Plant Biology, North Carolina State University, Raleigh, North Carolina 27695

^bDepartment of Pharmacology and Cancer Biology, Howard Hughes Medical Institute, Duke University Medical Center, Durham, North Carolina 27710

A genetic approach was used to increase phosphatidylinositol(4,5)bisphosphate [PtdIns(4,5)P₂] biosynthesis and test the hypothesis that PtdInsP kinase (PIPK) is flux limiting in the plant phosphoinositide (PI) pathway. Expressing human PIPK1 α in tobacco (*Nicotiana tabacum*) cells increased plasma membrane PtdIns(4,5)P₂ 100-fold. In vivo studies revealed that the rate of ³²Pi incorporation into whole-cell PtdIns(4,5)P₂ increased >12-fold, and the ratio of [³H]PtdInsP₂ to [³H]PtdInsP increased 6-fold, but PtdInsP levels did not decrease, indicating that PtdInsP biosynthesis was not limiting. Both [³H]inositol trisphosphate and [³H]inositol hexakisphosphate increased 3- and 1.5-fold, respectively, in the transgenic lines after 18 h of labeling. The inositol(1,4,5)trisphosphate [Ins(1,4,5)P₃] binding assay showed that total cellular Ins(1,4,5)P₃/g fresh weight was >40-fold higher in transgenic tobacco lines; however, even with this high steady state level of Ins(1,4,5)P₃, the pathway was not saturated. Stimulating transgenic cells with hyperosmotic stress led to another 2-fold increase, suggesting that the transgenic cells were in a constant state of PI stimulation. Furthermore, expressing Hs PIPK1 α increased sugar use and oxygen uptake. Our results demonstrate that PIPK is flux limiting and that this high rate of PI metabolism increased the energy demands in these cells.

INTRODUCTION

Inositol phospholipids are important for both sensing and responding to various stimuli in plants and animal cells. For example, phosphatidylinositol(4,5)bisphosphate [PtdIns(4,5)P₂] is the source of the second messenger inositol(1,4,5)trisphosphate [Ins(1,4,5)P₃], and it can directly affect the activity of membrane proteins, regulate cytoskeletal structure, and affect vesicle trafficking (for review, see Stevenson et al., 1998; Meijer and Munnik, 2003; Van Leeuwen et al., 2004). However, a long-standing mystery for plant scientists studying phosphoinositide (PI) signaling has been the low relative amount of PtdIns(4,5)P₂ in all terrestrial plants studied thus far (Gross and Boss, 1993; Munnik et al., 1998; Stevenson et al., 1998; Drøbak et al., 1999).

The ratio of [³H]inositol-labeled PtdIns(4)P to PtdIns(4,5)P₂ is usually on the order of 10:1, which is high compared with the 1:1 and 1:2 ratios characteristic of rapidly responding animal cells (Adel-Latif et al., 1985; Cunningham et al., 1995). The relatively low

steady state level of PtdIns(4,5)P₂ in plants could result from a low rate of phosphorylation of PtdIns(4)P by PtdIns(4)P 5-kinase to form PtdIns(4,5)P₂ or from rapid hydrolysis by phospholipase C (PLC) or dephosphorylation by a phosphatase (Drøbak et al., 1999; Pical et al., 1999; Stevenson et al., 2000; Berdy et al., 2001; DeWald et al., 2001; Burnette et al., 2003; Hunt et al., 2003; Ercetin and Gillaspay, 2004; Zhong et al., 2004; Williams et al., 2005).

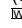
A clue as to the differences in plant and animal PI signaling came from studies of lipid kinase activities in membranes isolated from rats and plants (Sandelius and Sommarin, 1990). These early experiments revealed that rat plasma membranes had 20-fold higher specific activity relative to soybean (*Glycine max*) hypocotyl or wheat (*Triticum aestivum*) shoot plasma membranes. More recently, plant genes have been cloned and expressed as recombinant proteins for biochemical characterization (Mikami et al., 1998; Elge et al., 2001; Westergren et al., 2001; Perera et al., 2005). A kinetic analysis of two isoforms of *Arabidopsis thaliana* PtdInsP kinases (At PIPK1 and At PIPK10) indicated that the plant enzymes were significantly less active (V_{max}/K_m of 20- to 200-fold less, respectively) compared with the human enzyme, Hs PIPK1 α (Perera et al., 2005).

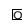
A unique feature of plant type I PIPKs is the presence of several MORN motifs in the N-terminal region of the protein. The N-terminal MORN domain is critical for regulating PIPK activity, and it affects membrane attachment in vivo (Im et al., 2007). Furthermore, PtdInsP kinase activity is regulated by protein phosphorylation (Westergren et al., 2001). These results clearly indicate that PtdInsP₂ synthesis in plants is under tight control.

¹ Current address: BASF Plant Science, 26 Davis Dr., Research Triangle Park, NC 27709.

² To whom correspondence should be addressed. E-mail wendy_boss@ncsu.edu; fax 919-515-3436.

The author responsible for distribution of materials integral to the findings presented in this article in accordance with the policy described in the Instructions for Authors (www.plantcell.org) is: Wendy F. Boss (wendy_boss@ncsu.edu).

 Online version contains Web-only data.

 Open Access articles can be viewed online without a subscription. www.plantcell.org/cgi/doi/10.1105/tpc.107.051367

It is also evident that maintaining normal/adequate PtdInsP₂ levels is important for different aspects of plant growth and development. For example, a continuous supply of PtdIns(4,5)P₂ mediated through PtdIns 4-kinase or lipid transfer proteins is essential for normal root hair growth (Vincent et al., 2005; Preuss et al., 2006). Furthermore, the PI phosphatase *sac9* mutant had 4-fold higher PtdInsP₂ levels in root tissue and decreased primary and lateral root growth (Williams et al., 2005). An *Arabidopsis* PIPK mutant *pip5k9-d* (which has a mutation in the 3' untranslated region of the gene, resulting in increased transcript levels) showed reduced primary root growth (Lou et al., 2007); however, it was not reported whether these changes were a result of changes in PtdInsP₂ levels. Finally, tip growth in pollen tubes is also dependent on PtdInsP₂ turnover (Dowd et al., 2006; Helling et al., 2006). These data suggest that the PI pathway is important for membrane trafficking and plasma membrane biogenesis.

In previous work, we found that plant cells transformed with the human type I InsP 5-phosphatase [which increased the rate of turnover of Ins(1,4,5)P₃] showed increased endogenous PIPK activity. However, PLC activity was not altered (Perera et al., 2002). These results led to the hypothesis that the phosphorylation of PtdIns(4)P by PtdIns(4)P 5-kinase is a flux-limiting step in the plant PI pathway. To test this hypothesis, we have taken a synthetic biology approach. Using a well-characterized model plant system with relatively low PtdIns(4,5)P₂, tobacco (*Nicotiana tabacum*) cells grown in suspension culture (Perera et al., 2002), we expressed a human PtdIns(4)P 5-kinase gene, Hs *PIP1K* α . We chose Hs *PIP1K* α because At *PIP1K* 1 and 10, the plant PIPKs characterized thus far, are much less active than Hs *PIP1K* α (Perera et al., 2005) and because Hs *PIP1K* α is a type I family PIPK (Kunz et al., 2000, 2002), which is functionally similar to the plant PIPKs (Mueller-Roeber and Pical, 2002). Importantly, Hs *PIP1K* α lacks MORN motifs; therefore, expressing Hs *PIP1K* α would increase PIPK activity without affecting MORN motif-interacting partners of At *PIP1K* 1-9. For comparison to the human enzyme, we have expressed At *PIP1K* 10, which does not contain MORN motifs.

In this article, we show that expressing Hs *PIP1K* α increases the plasma membrane PtdIns(4,5)P₂ 100-fold and generates a steady state increase in Ins(1,4,5)P₃ that is similar to what is experienced transiently upon stimulation in nontransformed cells. These insights reveal the impact of increased PtdInsP₂ biosynthesis on cellular metabolism. Because the transgenic cells are in a constant state of PI stimulation, they provide a good model for studying PI signaling.

RESULTS

Expression of PIPKs in Tobacco Cells

Vector constructs with either green fluorescent protein (GFP)-Hs *PIP1K* α , GFP-At *PIP1K* 10, or GFP alone were used for *Agrobacterium tumefaciens*-mediated transformation of the wild-type tobacco (NT-1) cells as previously described (Perera et al., 2002). Three independent lines producing GFP-Hs *PIP1K* α and GFP-At *PIP1K* 10 (hereafter referred to as Hs *PIP1K* α and At *PIP1K* 10) along with a GFP control line were selected for further study. Transcript levels were determined using gene-specific primers for GFP and the PIPKs (Figure 1A).

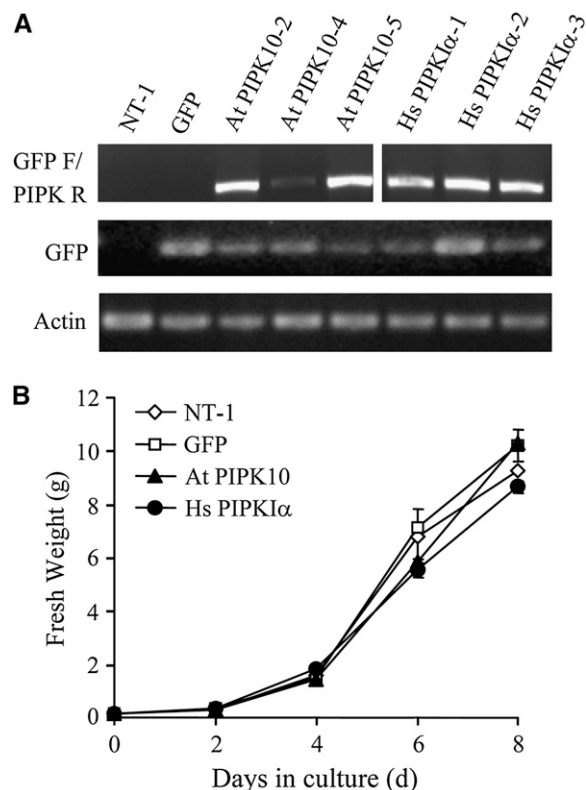


Figure 1. Expression of GFP-PtdInsP 5-Kinase Genes in the Transgenic Tobacco Cells.

(A) RT-PCR analysis. RNA was isolated from wild-type and transgenic tobacco cell lines harvested on day 4 of the culture cycle. Equal amounts of RNA from each sample were reverse transcribed and subjected to RT-PCR using GFP, PIPK, and actin-specific primers. The full-length fusion transcripts were identified with a combination of GFP forward and the selective kinase reverse primers (top panel). Amplification of actin is shown to indicate that equal amounts of RNA were used from each sample. NT-1 (wild type); GFP (GFP vector control); At *PIP1K* 10-2, At *PIP1K* 10-4, and At *PIP1K* 10-5 (three independent transgenic lines transformed with GFP fused to *Arabidopsis* *PIP1K* 10); Hs *PIP1K* α -1, Hs *PIP1K* α -2, and Hs *PIP1K* α -3 (three independent transgenic lines transformed with GFP fused to human *PIP1K* α).

(B) Growth curve of wild-type and transgenic cell lines over the culture cycle. The fresh weight of two replicate 25-mL cultures was measured on each day. The values are averages (SD) of duplicates from two experiments.

Cell growth was compared over the normal 7-d growth cycle (Figure 1B). For all subsequent experiments, cells were grown under similar conditions, and the fresh weight of wild-type and transgenic cell lines did not vary more than 10%.

Subcellular Distribution of the Recombinant GFP-PIPKs

To determine the subcellular distribution of the GFP-PIPK proteins, the cells were imaged using a confocal microscope. Fluorescence was visible throughout the cytosol and nucleus for the GFP-expressing tobacco cells (Figure 2A) as previously

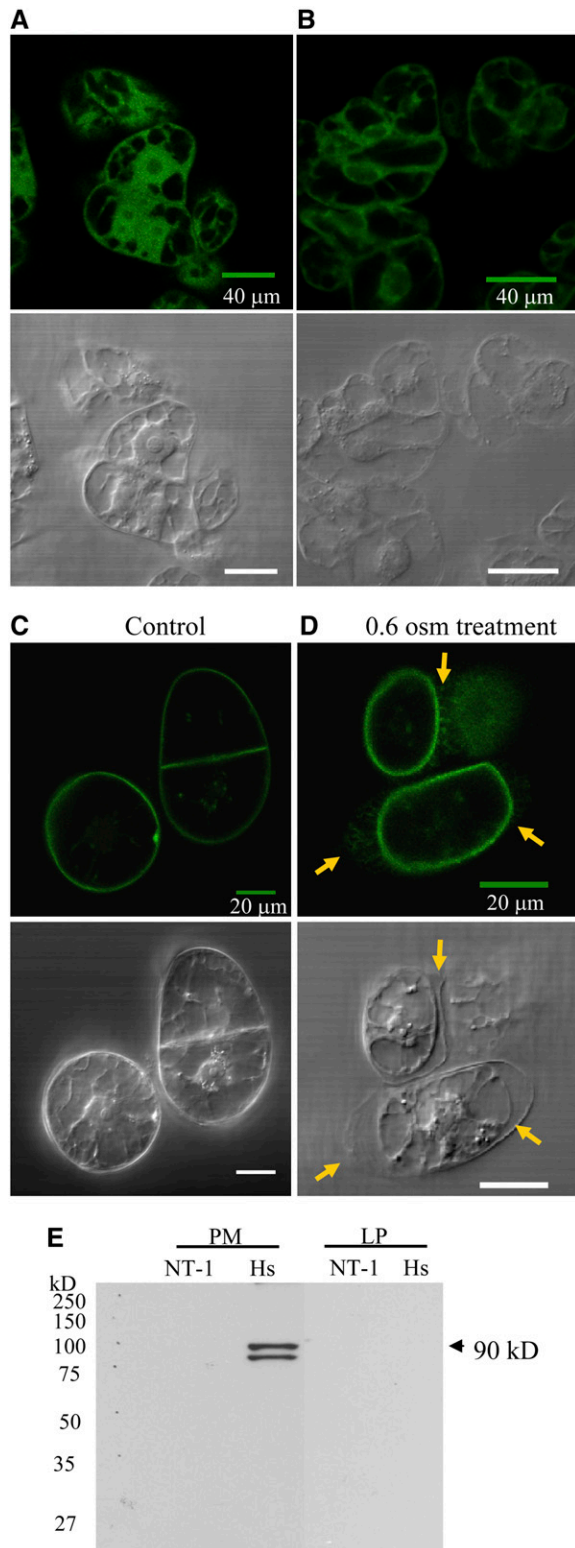


Figure 2. Full-Length GFP-Hs PIPK1 α Localized with the Plasma Membrane.

(A) to **(C)** Transgenic tobacco cells expressing *GFP* **(A)** and *GFP-At PIPK10* **(B)**, and *GFP-Hs PIPK1 α* **(C)** were imaged using a confocal

microscope. Top panels show fluorescence, and bottom panels show differential interference contrast images. **(D)** To confirm plasma membrane localization of Hs PIPK1 α , tobacco cells were treated with 0.6 osmolal sorbitol for 5 min. Arrows indicate the position of the cell wall. **(E)** Immunoblot of plasma membrane (PM) and lower-phase (LP) proteins using a monoclonal antibody raised against GFP. The antiserum recognizes a protein of ~ 90 kD (the predicted molecular weight of GFP-Hs PIPK1 α) and a lower band that may be a proteolytic product in the plasma membrane of Hs PIPK1 α cells. Equal amounts of membrane proteins were loaded from NT-1 (wild-type tobacco cells) and Hs (GFP-Hs PIPK1 α lines).

described (Haseloff and Amos, 1995; Persson et al., 2002). By contrast, At PIPK10 was detected throughout the cytoplasmic strands but not in the nucleus (Figure 2B), and Hs PIPK1 α was associated with the plasma membrane of the tobacco cells (Figure 2C; see Supplemental Video 1 online). To confirm plasma membrane localization of Hs PIPK1 α , tobacco cells were treated with 0.6 osmolal sorbitol for 5 min (Figure 2D). Note the fluorescence remains with the plasma membrane and can be seen on the Hechtian threads, plasma membrane extensions that remain tightly associated with the cell wall (indicated by the arrows in Figure 2D and in Supplemental Video 2 online).

Immunoblot analysis of proteins isolated from 4-d-old tobacco cells visualized with antiserum recognizing the GFP tag is shown in Figure 2E. Membranes were isolated by aqueous two-phase partitioning and proteins separated by gel electrophoresis. Hs PIPK1 α was detected at the predicted size of the protein (~ 90 kD) in the plasma membrane fraction and not in the lower phase membrane fraction by aqueous two-phase partitioning. These data confirmed that Hs PIPK1 α was localized to the plasma membrane. Unlike Hs PIPK1 α , At PIPK10 could not be detected by immunoblotting from a soluble, plasma membrane or lower-phase membrane fraction probably due to the low abundance of expressed protein (data not shown).

Expressing the PIPKs Increased PtdInsP 5-Kinase Activity and PtdIns(4,5)P₂

To determine whether expression of the At PIPK10 or Hs PIPK1 α increased PtdInsP 5-kinase activity in tobacco cells, we first measured the plasma membrane lipid kinase activity in vitro. Two- to 3-fold more [³²P]PtdIns(4,5)P₂ was formed by membranes from two independent Hs PIPK1 α lines even without adding exogenous PtdIns(4)P (Figure 3A). These data indicate that PtdIns(4)P was not limiting in the transgenic lines and that the human enzyme could phosphorylate the endogenous plant lipids. When PtdIns(4)P was added in excess, the specific activity of the isolated plasma membranes was 100-fold greater in the Hs PIPK1 α lines and 1.5- to 2-fold greater in the At PIPK10 lines compared with the untransformed NT-1 plasma membranes (Figure 3B).

Plant plasma membrane PtdInsP 5-kinase activity was reported previously to cosediment with the F-actin pellet isolated from carrot (*Daucus carota*) plasma membranes (Tan and Boss, 1992), and At PIPK1 has been shown to bind actin directly (Davis et al., 2007). With the wild-type tobacco cells, 66% \pm 6% of the

microscope. Top panels show fluorescence, and bottom panels show differential interference contrast images.

(D) To confirm plasma membrane localization of Hs PIPK1 α , tobacco cells were treated with 0.6 osmolal sorbitol for 5 min. Arrows indicate the position of the cell wall.

(E) Immunoblot of plasma membrane (PM) and lower-phase (LP) proteins using a monoclonal antibody raised against GFP. The antiserum recognizes a protein of ~ 90 kD (the predicted molecular weight of GFP-Hs PIPK1 α) and a lower band that may be a proteolytic product in the plasma membrane of Hs PIPK1 α cells. Equal amounts of membrane proteins were loaded from NT-1 (wild-type tobacco cells) and Hs (GFP-Hs PIPK1 α lines).

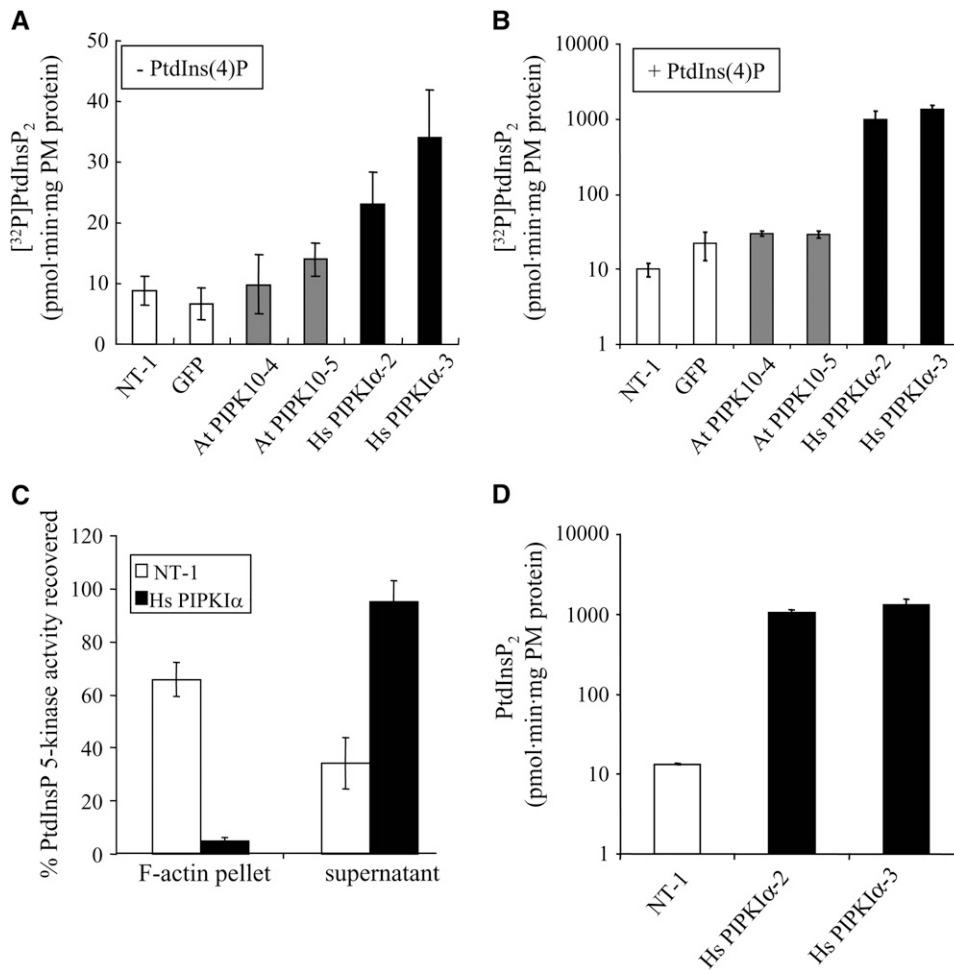


Figure 3. Plasma Membrane PtdInsP 5-Kinase-Specific Activity and PtdIns(4,5)P₂ Levels Increased >100-Fold in Hs PIPK1α Lines and Was Not Associated with Actin.

(A) and **(B)** The plasma membrane (PM)-enriched fraction from wild-type and two different lines of transgenic tobacco cells were analyzed for PtdInsP 5-kinase activity without **(A)** and with **(B)** added substrate, PtdIns(4)P.

(C) The PtdInsP 5-kinase activity recovered with F-actin polymerized and recovered in a 20,000g pellet from the plasma membrane of NT-1 and Hs PIPK1α lines was compared.

(D) Mass measurements of plasma membrane PtdIns(4,5)P₂ levels of wild-type and Hs PIPK1α lines. The values plotted are the averages ± SD of two to three independent experiments assayed in duplicate. Note the data in **(B)** and **(D)** are plotted on a log scale.

total plasma membrane PtdInsP 5-kinase activity cosedimented with the 20,000g F-actin pellet. However, of the plasma membrane PtdInsP 5-kinase activity from the Hs PIPK1α lines, 95% ± 8% was recovered in the detergent-soluble fraction and only 5% ± 1% sedimented with 20,000g F-actin pellet (Figure 3C). The fact that Hs PIPK1α did not cosediment with large F-actin bundles results from both the lack of the appropriate actin binding proteins necessary to form an Hs PIPK1α-actin scaffold and the inability of Hs PIPK1α to directly bind actin (Davis et al., 2007). The data confirm that Hs PIPK1α is associated with the plasma membrane and suggest that overproducing Hs PIPK1α should result in increased PtdIns(4,5)P₂ in the plasma membrane, unless catabolism by PLC or a lipid phosphatase is greater than the rate of synthesis.

To monitor endogenous levels of PtdIns(4,5)P₂ in the plasma membrane of transgenic tobacco cells *in vivo*, we used mass

measurement. For these analyses, lipids were extracted from isolated plasma membranes from wild-type and Hs PIPK1α lines, the head group was hydrolyzed, and the total Ins(1,4,5)P₃ released was monitored using the Ins(1,4,5)P₃ binding assay. The plasma membrane PtdIns(4,5)P₂ from the Hs PIPK1α lines increased >100-fold per mg membrane protein, from ~10 to 1000 pmol·mg protein (Figure 3D).

We also monitored steady state levels of the major phospholipids in the plasma membrane (Figure 4). Plasma membrane-enriched fractions were isolated from 4-d-old wild-type and transgenic tobacco cells and subjected to lipid extraction and profiling as described by Welti et al. (2002). The major structural lipids of the membrane, such as PtdGro, PtdEtn, PtdIns, PtdCho, and PtdSer, were not significantly different between wild-type and Hs PIPK1α cells. The most significant difference was the

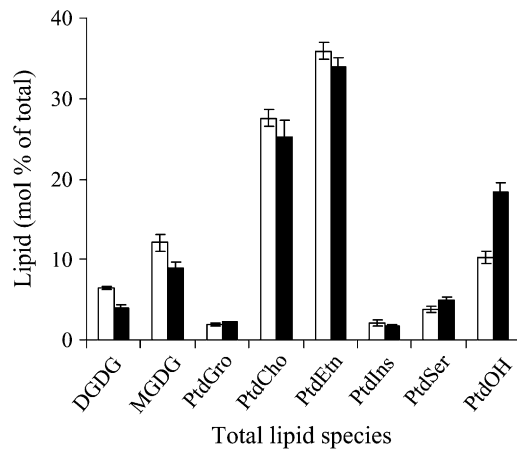


Figure 4. Polar Lipid Classes (Mol % of Total Polar Glycerolipids Analyzed) in the Plasma Membrane of Wild-Type and Hs PIPK α Lines.

The major phospholipid classes (phosphatidylcholine [PtdCho], phosphatidylethanolamine [PtdEtn], phosphatidylglycerol [PtdGro], and phosphatidylinositol [PtdIns]), galactolipid classes (monogalactosyldiacylglycerol [MGDG] and digalactosyldiacylglycerol [DGDG]), and minor phospholipid classes (phosphatidylserine [PtdSer] and phosphatidic acid [PtdOH]) were present. Values are average \pm SE of duplicates from three independent experiments. Open bars, wild-type lines; closed bars, Hs PIPK α lines.

\sim 1.8-fold increase in PtdOH in the Hs PIPK α cells. In addition to the phospholipids, the plasma membrane digalactosyldiacylglycerol and monogalactosyldiacylglycerol levels were decreased by \sim 30% in the Hs PIPK α cells compared with the wild type.

Increased Turnover of PI Pathway Intermediates and Increased Rate of PtdInsP $_2$ Synthesis in Vivo

To monitor the levels of intermediates in the PI pathway, tobacco cells were labeled in vivo with [3 H]inositol (Table 1). Even though 20% of [3 H]inositol can be incorporated into pectin and other cell wall polysaccharides (Verma and Maclachlan, 1976), in vivo labeling will give a relative measure of pool sizes for the major components of the PI pathway. The ratio of PtdIns(4)P to PtdIns(4,5)P $_2$ in wild-type tobacco cells was \geq 10:1. Expression

of Hs PIPK α increased the total cellular [3 H]PtdIns(4,5)P $_2$, and the ratio of [3 H]PtdIns(4)P to [3 H]PtdIns(4,5)P $_2$ decreased to 2:1 without decreasing the total [3 H]PtdIns(4)P. Analysis of the glycerophosphoinositol head groups confirmed the presence PtdIns4P and PtdIns(4,5)P $_2$ (see Supplemental Figure 1 online). These data indicate that the PtdIns(4)P pool can be maintained at an adequate level to meet the demands of the increased PtdIns(4,5)P $_2$ biosynthesis. It also supports the hypothesis that under normal conditions, PIPK activity is a flux-limiting step in the PI pathway of the wild-type cells.

The rate of [32 P]PtdIns(4,5)P $_2$ biosynthesis in vivo was measured by adding 32 Pi to 4-d-old transgenic Hs PIPK α and wild-type tobacco cells preequilibrated in conditioned medium. Cells were harvested at each time point, and whole-cell lipids were extracted and separated by thin layer chromatography (TLC) (Figure 5A). Typically, little [32 P]PtdIns(4,5)P $_2$ was detected in the nontransformed cells. The incorporation of 32 Pi into PtdIns(4,5)P $_2$ in Hs PIPK α lines was 12-fold higher than wild-type cells (Figure 5B) and saturated by 4 min when calculated as total [32 P]-labeled lipids. The incorporation of 32 Pi into PtdInsP was \sim 20% less in Hs PIPK α lines when calculated as percentage total [32 P]-labeled lipids (Figure 5C). This reflects the high percentage of [32 P]PtdIns(4,5)P $_2$ and the rapid conversion of [32 P]PtdInsP to [32 P]PtdIns(4,5)P $_2$. Comparison of these data with long-term [3 H] labeling indicates that de novo synthesis of [3 H]PtdInsP from intracellular pools was adequate to sustain [3 H] PtdIns(4,5)P $_2$ biosynthesis.

As expected, in both cell lines, the [32 P]PtdInsP decreased with time as the total percentage of [32 P]-labeled phospholipids because of the increased incorporation of [32 P] into PtdCho and PtdEtn. The observation that similar amounts of whole-cell [32 P]PtdOH formed in all lines (Figure 5D) is a good indication that the cells were not stressed during the labeling (Walti et al., 2002) and that the increases in 32 Pi incorporation were specific for PtdIns(4,5)P $_2$.

Expressing the PIPKs Increased the Steady State Ins(1,4,5)P $_3$

To determine whether increasing the rate of synthesis and the total mass of PtdIns(4,5)P $_2$ in the plasma membranes would affect the total cellular Ins(1,4,5)P $_3$, Ins(1,4,5)P $_3$ levels were measured in wild-type and PIPK transgenic lines using the

Table 1. Analysis of the [3 H] Inositol Lipids from Wild-Type (NT-1) and Transgenic Tobacco Cells Expressing PIPKs

Cell Type	[3 H] Inositol-Labeled Phospholipids			Ratio PtdInsP/PtdInsP $_2$
	(Percentage of Total [3 H] Lipid Recovered)			
	PtdIns	PtdInsP	PtdInsP $_2$	
NT-1	91 \pm 0.9	2.7 \pm 0.9	0.24 \pm 0.09	12:1
GFP	89 \pm 1.2	3.0 \pm 0.7	0.20 \pm 0.07	15:1
At PIPK10	88 \pm 1.2	3.2 \pm 0.5	0.27 \pm 0.06	12:1
Hs PIPK α	87 \pm 1.5	2.4 \pm 0.5	1.70 \pm 0.90	2:1

Tobacco cells were labeled in vivo with *myo*-[3 H]inositol for 24 h, and the lipids were extracted and separated by TLC. The values for [3 H] labeled PtdIns, PtdInsP, and PtdInsP $_2$ are the percentage of total radioactivity recovered (averages \pm SD of two independent experiments assayed in duplicate).

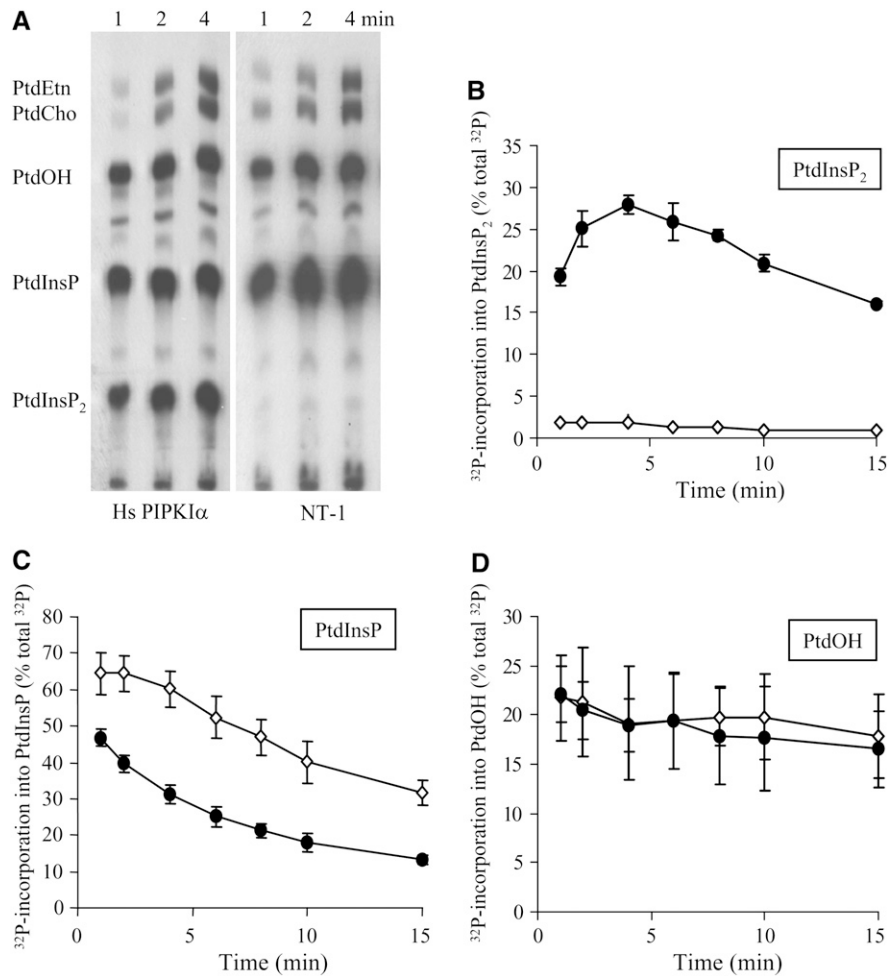


Figure 5. In Vivo Labeling with $^{32}\text{P}_i$ Indicates a Rapid Rate of [^{32}P]PtdInsP₂ Biosynthesis in the Hs PIPK1 α Lines.

All cells were preequilibrated in conditioned medium for 30 min; $^{32}\text{P}_i$ was added, cells were harvested, and lipids were extracted at the time points indicated. The lipids were separated by TLC, and ^{32}P -labeled lipids were quantified with a Bioscan imaging scanner.

(A) Representative autoradiogram of the TLC plate.

(B) to (D) ^{32}P recovered phospholipids (PtdInsP₂, PtdInsP, and PtdOH, respectively) over the time course (wild type, open diamonds; Hs PIPK1 α lines, closed circles). The data are reported as percentage of total cpm recovered per lane. Each point is the average \pm SD of duplicates from three independent experiments.

Ins(1,4,5)P₃ binding assay (Table 2). In the Hs PIPK1 α lines, the cellular Ins(1,4,5)P₃ was >40-fold higher than that of the wild-type lines, and in the At PIPK10 lines, the total cellular Ins(1,4,5)P₃ was 1.5- to 2-fold higher based on the Ins(1,4,5)P₃ binding assay.

When the cells were stimulated by a hyperosmotic stress of 0.6 osmolar sorbitol, the total Ins(1,4,5)P₃ was higher in all cell lines (Table 2). Ins(1,4,5)P₃ levels in the unstimulated Hs PIPK1 α lines were in a similar range to those of the stimulated nontransformed lines. In spite of these high levels, the Ins(1,4,5)P₃ increased >2.5-fold when the Hs PIPK1 α lines were stimulated. These data indicated that the capacity to hydrolyze PtdIns(4,5)P₂ by PLC was not saturated in the Hs PIPK1 α lines and indicate that the cells are in a continuously stimulated state with regard to PI signaling.

To compare the relative levels of [^3H]inositol phosphates, cells were labeled with *myo*-[2- ^3H]inositol for 18 h, and water-soluble

inositol phosphates were extracted and separated by HPLC. In addition to the increase in [^3H]InsP₃, [^3H]InsP₆ also was significantly higher in the Hs PIPK1 α lines (Table 3).

Cells with Increased PI Turnover Require More Calcium to Grow

The increased flux through the PI pathway and constantly high Ins(1,4,5)P₃ in the Hs PIPK1 α lines should mobilize and may deplete the intracellular calcium stores. If the calcium stores were depleted, it might be expected that the Hs PIPK1 α cells would grow less in medium with low calcium since calcium is essential for growth (Persson et al., 2001; Wu et al., 2002; Cheng et al., 2005). Cell growth was compared over the growth cycle in culture medium lacking calcium. While wild-type NT-1 cells grow

Table 2. Basal Ins(1,4,5)P₃ Was >40-Fold Higher in the Hs PIPK1 α Cells and Increased Further in Response to Osmotic Stress

Cell Type	Control (pmol InsP ₃ /g FW)	Osmotic Stress (pmol InsP ₃ /g FW)	Fold Increase in InsP ₃
NT-1	139 \pm 57	3,099 \pm 366	25.5 \pm 11.0
GFP	138 \pm 47	4,336 \pm 327	34.6 \pm 6.0
At PIPK10-4	328 \pm 125	3,252 \pm 1,145	10.1 \pm 0.5
At PIPK10-5	239 \pm 4	2,442 \pm 229	10.2 \pm 3.0
Hs PIPK1 α -2	6,457 \pm 1,692	16,679 \pm 4,598	2.6 \pm 0.1
Hs PIPK1 α -3	5,260 \pm 106	13,427 \pm 4,893	3.7 \pm 1.4

Cells (0.25 g fresh weight [FW]) were preequilibrated in 5 mL of conditioned medium and harvested at time zero (control) and 15 min after adding 0.6 osmolal sorbitol. Ins(1,4,5)P₃ was quantified using the Ins(1,4,5)P₃ binding assay. Data are the averages \pm SD from three separate experiments.

less without added calcium in the medium (compared with normal medium, Figure 1B, which contains 3 mM Ca²⁺), the Hs PIPK1 α cells did not grow at all without added Ca²⁺ (Figure 6A). These data suggested that the Hs PIPK1 α cells lacked the calcium reserves of the wild-type cells.

The endoplasmic reticulum (ER) chaperones and calcium binding proteins, calreticulin (CRT) and binding protein (BiP), will bind endogenous calcium (Lievremont et al., 1997; Michalak et al., 1999). There was a significant increase in both CRT and BiP in the Hs PIPK1 α lines in cells grown in normal medium with 3 mM calcium (Figure 6B). CRT increases with ER stress and when overproduced will increase ER-Ca²⁺ stores (Michalak et al., 1999; Persson et al., 2001; Akesson et al., 2005). The fact that the Hs PIPK1 α lines did not grow on low Ca²⁺ medium suggests that they had low not high Ca²⁺ reserves (Wu et al., 2002; Cheng et al., 2005) and that the increase in CRT reflects an effort by the cells to bind and retain the remaining Ca²⁺ against the constant stimulus.

In vitro assays indicated that both ER and mitochondrial fractions from the Hs PIPK1 α cells showed a 2-fold increase in [⁴⁵Ca²⁺] uptake compared with the wild-type cells (Figure 6C; see Supplemental Figure 2A online). The enhanced uptake in the in vitro assays is consistent with the depletion of endogenous stored Ca²⁺ (i.e., increased number of available Ca²⁺ binding sites). After 20 min when [⁴⁵Ca²⁺] uptake reached equilibrium, the Ca²⁺/H⁺ ionophore, ionomycin, was added to the membranes to release the ER-accumulated Ca²⁺ pool. As seen in Figure 6D, the ionomycin-released Ca²⁺ was \sim 2.5 to 3-fold higher in Hs PIPK1 α cells compared with the wild type. This increase in ionomycin-releasable Ca²⁺ is similar to that observed

when CRT was overexpressed in NT-1 cells and is consistent with Ca²⁺ binding to the low-affinity binding sites on CRT (Persson et al., 2001).

An increase in Ca²⁺ flux also was detected in in vivo labeling studies using whole cells. If exposed to [⁴⁵Ca²⁺], the Hs PIPK1 α cells took up slightly more [⁴⁵Ca²⁺] than wild-type cells (see Supplemental Figure 2B online). The growth study and [⁴⁵Ca²⁺] data indicate that while the Hs PIPK1 α cells have increased their capacity to store calcium, because of the constitutively high levels of InsP₃, there will be a net efflux of Ca²⁺ and the cells require more exogenous calcium to survive.

We were unable to detect significant differences in cytosolic free calcium in whole cells using Indo-1 to monitor free calcium (see Supplemental Figure 3 online). When we measured total cellular Ca²⁺ using inductively coupled plasma (ICP) emission spectrometry, the Hs PIPK1 α cells had 15.7% \pm 1.1% and 15.6% \pm 6.8% less Ca²⁺ per g dry weight at 4 and 6 d, respectively, compared with the NT-1 cells (values are the average of four numbers from two experiments). The combination of in vitro and in vivo measurements makes a compelling argument that the increase in PI metabolism in the Hs PIPK1 α cells has increased the flux of Ca²⁺, resulting in a net loss of cellular Ca²⁺ and depletion of intracellular stores.

Increasing the Flux through the PI Pathway Increases Basal Metabolism

PtdIns(4,5)P₂ biosynthesis from PtdIns requires two molecules of ATP; therefore, rapid turnover of the PI pathway should increase the demand for ATP (Poggioli et al., 1983; Yeung et al., 2006). In addition, InsP₆ may be synthesized in plants by multiple routes that require ATP (Brearley and Hanke, 1996; Phillippy, 1998; Raboy, 2001; Stevenson-Paulik et al., 2002). Our in vivo labeling data provide support for the sequential phosphorylation of Ins(1,4,5)P₃ to Ins(1,2,3,4,5,6)P₆. This increased demand for ATP and an increased demand for energy as a result of increased Ca²⁺ flux should increase respiration in the transgenic tobacco cells. To monitor respiration in vivo, we used a Clarke oxygen electrode and measured oxygen uptake over time. As shown in Table 4, oxygen uptake by whole cells increased 40% in the Hs PIPK1 α line. Although the trend was consistently higher, the increase in oxygen uptake in the At PIPK10 line was not statistically significant when averaged between experiments. With all cell lines, O₂ uptake was completely inhibited by iodoacetate, a general inhibitor that also inhibits glycolysis (data not shown).

Table 3. Hs PIPK1 α Lines Produced More [³H]InsPx

Cell Type	[³ H] Inositol Phosphates (Percentage of Total [³ H]InsPx Recovered from Water-Soluble Fraction)			
	InsP ₂	InsP ₃	InsP ₅	InsP ₆
NT-1	8.1 \pm 0.2	0.6 \pm 0.1	0.7 \pm 0.3	6.4 \pm 0.2
GFP	7.3 \pm 0.3	0.7 \pm 0.2	1.2 \pm 0.4	6.6 \pm 0.3
Hs PIPK1 α	6.7 \pm 0.7	2.0 \pm 0.3	1.1 \pm 0.7	9.4 \pm 1.0

To analyze the inositol phosphates from wild-type (NT-1) and transgenic cell lines, tobacco cells were labeled in vivo with *myo*-[2-³H]inositol for 18 h, and the water-soluble inositol phosphates were separated by HPLC and analyzed. [³H]InsP₄ was not detected.

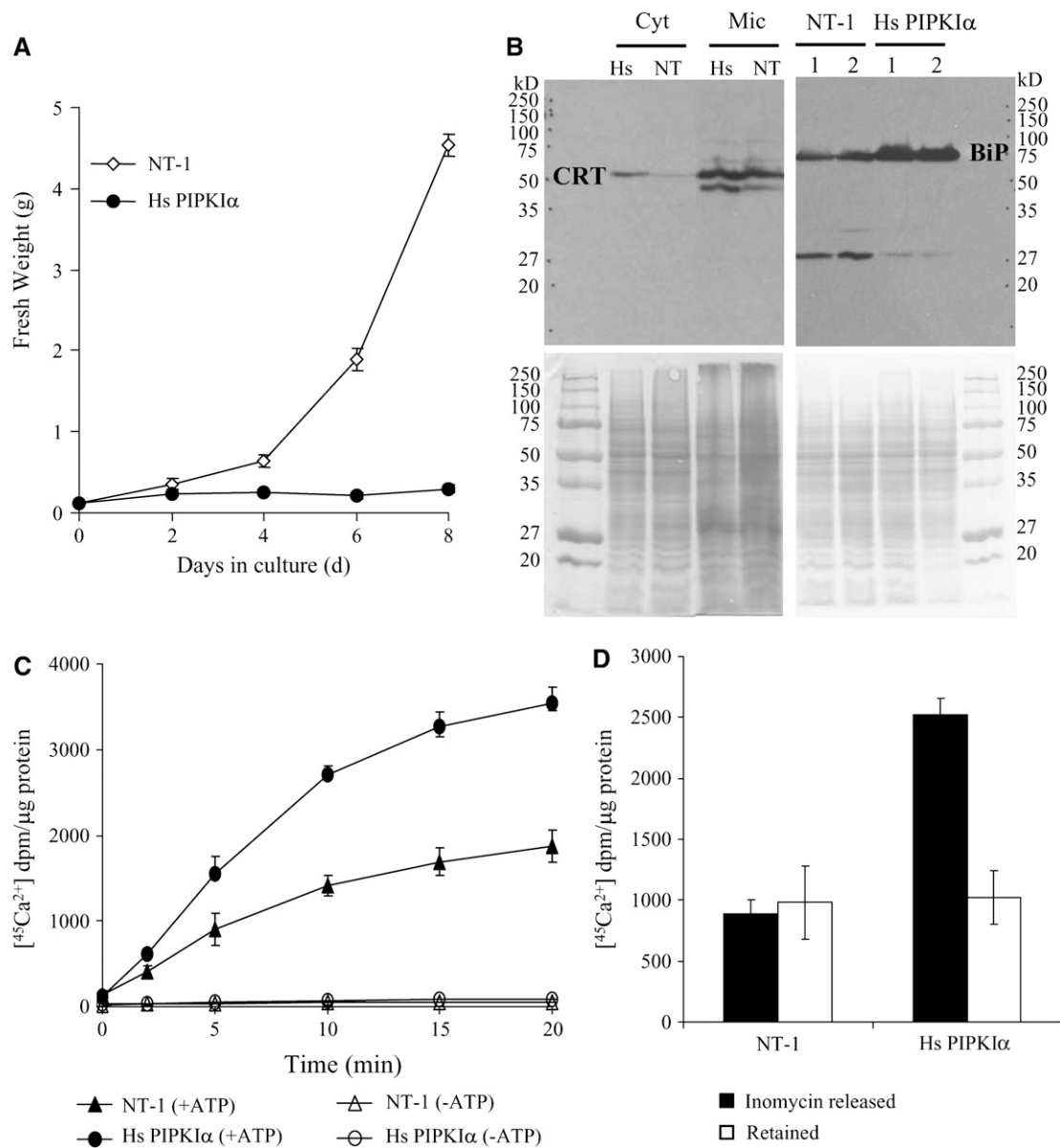


Figure 6. Hs PIPK1 α Lines Did Not Grow in Medium with No Added Calcium and Showed Signs of Changes in Calcium Homeostasis.

(A) Cells (0.25 g/fresh weight) were transferred to 25 mL of fresh medium without added calcium, and fresh weight was monitored every 2 d (wild type, open diamonds; Hs PIPK1 α lines, closed circles). The values are averages \pm SD of duplicates from two experiments.

(B) Hs PIPK1 α cells have increased CRT and BiP. Microsomal membranes (Mic) and cytosolic (Cyt) proteins were prepared from indicated cell lines, and 10 and 30 μ g of protein were separated by SDS-PAGE as noted. The calcium binding proteins CRT and BiP were detected with antibodies by immunoblotting as indicated.

(C) Increased Ca²⁺ uptake in ER from Hs PIPK1 α cells. ER-enriched membrane vesicles were prepared from the wild type (triangles) and Hs PIPK1 α (circles) as previously described (Persson et al., 2001). [⁴⁵Ca²⁺] (2 μ Ci) was added, and uptake was monitored. The ATP-dependent [⁴⁵Ca²⁺] uptake (10 μ g protein aliquot⁻¹) was measured in the presence (closed symbols) and absence (open symbols) of 3 mM ATP. The radioactivity was measured in a scintillation counter. Data are averages \pm SD of duplicates from two independent experiments.

(D) Hs PIPK1 α cells released more ER [⁴⁵Ca²⁺]. The Ca²⁺ ionophore ionomycin (1.5 μ M) was added to [⁴⁵Ca²⁺]-loaded ER-enriched membrane vesicles (23 min), and membrane vesicles were analyzed for [⁴⁵Ca²⁺] after 5 min. Closed bars, [⁴⁵Ca²⁺] released; open bars, [⁴⁵Ca²⁺] retained by the ER-enriched membranes. The values are averages \pm SD of duplicates from two experiments.

The mitochondria of the wild-type and transgenic cells were visualized with Rhodamine 123 (see Supplemental Figure 4 online). There was no marked increase in the number of mitochondria and no difference in O₂ uptake of isolated mitochondria (data not shown). Based on these observations, we hypothesized that the rate of glycolysis increased in the Hs PIPK1 α line due to the increased PtdIns(4,5)P₂ biosynthesis. If this were true, then the Hs PIPK1 α line should use up the sugar from the culture medium faster. Analysis of the sugar in the culture medium supported this hypothesis. At day 6, there was half as much sugar remaining in the medium of the Hs PIPK1 α lines compared with wild-type and GFP control lines (Table 5).

DISCUSSION

Our first goal was to test the hypothesis that phosphorylation of PtdIns(4)P to form PtdIns(4,5)P₂ by a PtdIns(4)P 5-kinase is a limiting step in plant PI metabolism. We showed that even though PtdIns(4)P is present and can be phosphorylated, the endogenous plant PIPKs are not as effective as the animal enzyme and that these differences are the main reason for the high ratio of PtdIns(4)P to PtdIns(4,5)P₂ found in terrestrial plants.

Our second goal was to increase the flux through the PI pathway to characterize the impact of increased PI signaling in a plant system. There were several advantages in using the human PtdIns(4)P 5-kinase, Hs PIPK1 α , for increasing PtdIns(4,5)P₂ in vivo: (1) Hs PIPK1 α has a low K_m for PtdIns(4)P and high V_{max} compared with the plant kinases characterized thus far (Perera et al., 2005); (2) the preferred substrate is PtdIns(4)P, which is similar to plant lipid kinases (Westergren et al., 1999, 2001; Kunz et al., 2000, 2002; Perera et al., 2005); (3) Hs PIPK1 α localized primarily with the plasma membrane in the tobacco cells, which means that it should directly affect the plasma membrane PtdIns(4,5)P₂ pools; (4) readily detectable amounts of enzyme were produced in the transgenic cells unlike overexpression of At PIPK10; (5) Hs PIPK1 α did not bind the actin cytoskeleton because the necessary human scaffolding proteins were not present in plants; (6) Hs PIPK1 α does not contain MORN motifs so that additional effects of the MORN motifs found in At PIPK1-9 would not impact the interpretation of our results; and (7) by increasing the rate of one enzymatic reaction, we could alter the metabolic flux through the pathway.

We initially attempted to use At PIPK1 for this work; however, constitutive expression of At PIPK1 did not result in any detectable increase in functional protein or enzyme activity. We suspect that the inability to overproduce this enzyme in plants may

Table 4. Cellular Respiration Increases in the Hs PIPK1 α Lines

Cell Type	nmoles O ₂ Taken up/min	Increased O ₂ Uptake (%)
NT-1	8 ± 3	–
GFP	8 ± 3	–
At PIPK10	11 ± 2	26
Hs PIPK1 α	13 ± 3	46

O₂ uptake was monitored using a Clarke electrode in fresh medium. The numbers are the averages ± SD from three independent experiments.

Table 5. Hs PIPK1 α Lines Deplete the Sugar from the Medium Faster

Cell Type	μ g of Sugar/mL Conditioned Media	
	4 d	6 d
NT-1	18.2 ± 0.1	6.2 ± 0.1
GFP	17.9 ± 0.4	6.0 ± 0.1
At PIPK10	16.8 ± 1.2	6.9 ± 0.1
Hs PIPK1 α	17.1 ± 0.1	3.4 ± 0.1

Sugar remaining in the culture medium was measured at the indicated day after transfer using Anthrone reagent as described in Methods. Data are the averages ± SD of duplicate values from two independent experiments.

result from the presence of the N-terminal MORN motifs or the actin binding domain in the linker region (Davis et al., 2007; Im et al., 2007). At PIPK10, which does not contain N-terminal MORN motifs or a linker region, can be overproduced. At PIPK10 increased PtdInsP₂ biosynthesis and the flux through the pathway as predicted; however, the At PIPK10-induced changes in PI metabolism were marginal compared with those imparted by the more active enzyme Hs PIPK1 α .

Tobacco cells expressing Hs PIPK1 α had a 100-fold increase in their plasma membrane PtdInsP₂ and a >40-fold increase in basal InsP₃ based on mass assays. A combinatorial approach including in vitro characterization of plasma membrane enzyme activity and in vivo short- and long-term labeling studies indicated that the tobacco cells had sufficient PtdIns(4)P substrate to sustain a high rate of PtdIns(4,5)P₂ biosynthesis. Furthermore, by increasing PtdIns(4,5)P₂ biosynthesis, we increased total cellular Ins(1,4,5)P₃. These data support our thesis that PtdInsP 5-kinase activity is a flux-limiting step in the plant PI pathway.

Profiling the plasma membrane lipids using electrospray ionization tandem mass spectrometry indicated that PtdOH levels were increased in the Hs PIPK1 α lines. The simplest explanation for this increase is that diacylglycerol produced by PLC activity is phosphorylated by diacylglycerol kinase; however, we did not detect appreciable differences in PtdOH production with short-term [³²P] labeling of whole cells. Alternatively, the increase in plasma membrane PtdOH in the Hs PIPK1 α lines may result from increased PLD activity. Selective plant PLDs isoforms are activated by Ca²⁺ and PtdInsP₂ (Pappan and Wang, 1999; Wang, 2000; Wang and Wang, 2001).

The impact of increased PtdIns(4,5)P₂ biosynthesis was manifested in basal cellular metabolism. Previous work with animal cells indicated that PtdIns(4,5)P₂ biosynthesis was completely inhibited by adding antimycin A and other inhibitors of mitochondrial respiration (Poggioli et al., 1983; Yeung et al., 2006). Changes in cytosolic calcium can directly affect mitochondria and stimulate respiration (McCormack et al., 1990; McCormack and Denton, 1993). It has been estimated that mitochondria can store up to 60% of the cellular calcium in some plant cells (Subbaiah et al., 1998; Logan and Knight, 2003). These data made a compelling argument that increasing PtdIns(4,5)P₂ turnover might put a significant demand on ATP biosynthesis. The increased use of sugar from the culture medium and increased oxygen uptake in the Hs PIPK1 α lines in conjunction with these previous studies in animal cells suggest that the status of

PtdIns(4,5)P₂ biosynthesis reflects the energy status of the cell. We also consistently observed a 30% increase in the plasma membrane vanadate-sensitive ATPase activity (data not shown). Taken together, the data indicate that when stimuli induce an increase in the PI pathway in plants, there will be an increased demand for ATP as the system responds and then recovers the PI pools to a prestimulated state.

If Ins(1,4,5)P₃ increases cytosolic calcium in plants as predicted based on early microinjection experiments (Gilroy et al., 1990; Tucker and Boss, 1996), then there must be a continuous and rapid transport of Ca²⁺ out of the cells or into intracellular stores to retain homeostasis in the Hs PIPK1 α lines. We observed an increase in ER calcium binding proteins, CRT and BiP, in the Hs PIPK1 α lines, indicating that the ER is sensing a change in calcium homeostasis. Furthermore, the fact that the Hs PIPK1 α lines required more extracellular Ca²⁺ to survive and that the ICP measurements indicated less total Ca²⁺/g dry weight suggests that the intracellular stores were depleted (Wu et al., 2002; Cheng et al., 2005). We cannot rule out the possibility that cell wall composition and therefore Ca²⁺ binding capacity is also compromised in the Hs PIPK1 α lines. The *fra3* mutants, which have increased PtdIns(4,5)P₂ resulting from a mutation in type II InsP 5-ptase, had thinner cell walls (Zhong et al., 2004).

What is the expected consequence of increasing the plasma membrane PtdIns(4,5)P₂ 100-fold? A large increase in negative charge on the inner leaflet of the plasma membrane would be expected to affect lipid and protein interactions and alter cell structure and membrane biogenesis (Yeung et al., 2006). Increasing plasma membrane PtdIns(4,5)P₂ has also been shown to generate actin comet tails and stress fibers and disrupt membrane trafficking in some animal cells (Rozelle et al., 2000; Yamamoto and Kiss, 2002; Kanzaki et al., 2004). We did not detect measurable differences in F-actin morphology based on phalloidin staining in the tobacco cells (see Supplemental Figure 5 online). This may be because the actin binding proteins required to scaffold Hs PIPK1 α to actin were not present in the plant cells (Ridley, 2006; Davis et al., 2007). The intensity of phalloidin staining appeared to be consistently greater in the Hs PIPK1 α lines, suggesting increased membrane permeability to phalloidin or possibly an increase in cable thickness reminiscent of the *Arabidopsis fra3* mutant. However, even though actin filaments in the *fra3* mutant were thickened and somewhat distorted, there was no evidence of actin comet tails (Zhong et al., 2004). Taken together with our observations that the plasma membrane PtdIns(4,5)P₂ was increased even higher in the Hs PIPK1 α lines than in the *fra3* mutants, these data suggest that PtdIns(4,5)P₂-mediated regulation of the actin cytoskeleton may be different in plant and animal cells (Davis et al., 2007).

The impact of increasing the flux through the pathway by increasing the rate PtdIns(4,5)P₂ biosynthesis is understandably different from mutating, silencing, or knocking out a selective gene in the PI pathway (Burnette et al., 2003; Hunt et al., 2003; Zhong et al., 2004; Williams et al., 2005). Manipulating PI metabolism/turnover/signaling at different steps in the PI pathway could lead to different physiological consequences. In previous work (Perera et al., 2002, 2006), we showed that dampening the Ins(1,4,5)P₃ signal and altering the flux by pulling metabolites through the PI pathway did not affect normal plant growth under

optimal conditions but rather delayed and reduced gravitropic bending in *Arabidopsis*, which is consistent with the dampened signal (Perera et al., 2006). The data also indicate that plants have compensatory mechanisms for sensing environmental cues and that InsP₃-mediated signaling can contribute to ~30% of the normal gravity signal. By overexpressing Hs PIPK1 α in this work, we have effectively pushed metabolites through the PI pathway and created plant cells that in theory should have reached a new steady state that is more similar to the rate of PI metabolism found in stimulated plant cells with InsP₃ providing a greater portion of the input signal.

We show that fundamental metabolic pathways were altered in the Hs PIPK1 α cells, including sugar use, respiration, and calcium homeostasis. These results emphasize the need to consider the impact of the turnover of second messengers on basal metabolism. Both transient or prolonged increases (15 min to several hours) in Ins(1,4,5)P₃ have been documented in response to gravistimulation and osmotic stress (Perera et al., 1999; DeWald et al., 2001) and may have important downstream consequences (such as different Ca²⁺ signatures). The generation of constitutively stimulated plant cells provides a unique system for characterizing the physiological impact of PI signaling in plants.

The synthetic model system presented here provides some insights as to the consequences of PI signaling in a stimulated plant cell. Taken together with previously published data (Perera et al., 2002, 2005, 2006; Im et al., 2007), this work demonstrates that in normal plant cells, PIPK activity is flux limiting. To understand the system and eventually develop a predictive model, it is important to appreciate the flux-limiting step and the consequences of altering plant PI metabolism.

METHODS

Plant Material and Growth

Tobacco cells (*Nicotiana tabacum* NT-1 cells) were maintained in 25 mL of liquid culture medium as described previously (Perera et al., 2002) and subcultured weekly with a 6% (v/v) inoculum. To monitor cell growth, two replicate 25-mL cultures grown in 125-mL Erlenmeyer flasks at 125 rpm and 27°C were harvested at 2, 4, and 6 d after transfer. The cells were collected by low-speed centrifugation (~500g for 3 min), and the fresh weight was measured. Cells were used 4 d after transfer unless otherwise indicated, and the average fresh weight harvested for both the wild-type and transgenic tobacco lines was 1.6 ± 0.2 g. For growth experiments with no added Ca²⁺, the tobacco culture media was made up with Murashige and Skoog salts except for the omission of Ca²⁺ salts.

Plant Transformation and Selection of Transgenic Lines

The cDNA encoding the At PIPK10 (At4g01190) and human PIPK1 α (NM_003557) were subcloned into the pENTR/SD/D-TOPO destination vectors (Invitrogen) and then into pK7WGF2 (Functional Genomics Division of the Department of Plant Systems Biology, Gent, Belgium) for production of GFP fusion PIPK proteins under the control of a cauliflower mosaic virus 35S promoter in plants by LR recombination reaction according to the manufacturer's instructions (Invitrogen). The orientation of the resulting plasmids, pK7WGF2-PIPks, was verified by PCR and DNA sequencing.

The recombinant binary plasmids (pK7WGF2-At PIPK10, pK7WGF2-Hs PIPK1 α , and vector control pK7WGF2) were transformed into

Agrobacterium tumefaciens EHA105 by the freeze-thaw method (Chen et al., 1994). NT-1 cells were transformed using *Agrobacterium*-mediated gene transfer as described (Perera et al., 2002). For each transformation, three independent, kanamycin-resistant microcalli were selected, and suspension cultures were established and maintained by weekly subculture in NT-1 medium containing 50 $\mu\text{g mL}^{-1}$ kanamycin.

RNA Extraction and RT-PCR Analysis

To verify transformation and determine if the transgene was expressed, three independent transformed NT-1 lines/constructs were harvested after 4 d of growth and frozen in liquid N_2 . RNA was isolated using the plant RNeasy kit (Qiagen), with an additional DNase treatment to remove contaminating genomic DNA. Reverse transcription was performed using Omniscript reverse transcriptase enzyme according to the manufacturer's instructions (Qiagen). GFP-PIPK transcripts were detected by PCR using a forward primer to GFP and PIPK-specific reverse primers. PCR with actin-specific primers was performed to verify that an equal amount of template was used. PCR products were analyzed by gel electrophoresis.

Microscopy

Confocal fluorescence images were acquired with a Leica TCS SP1 confocal system using a Leica DM IRBE microscope and a $\times 40$ numerical aperture 1.2 oil immersion objective. For GFP visualization, samples were excited with an argon laser at 488 nm, and fluorescence emission was collected from 500 to 560 nm. To visualize mitochondria, cells were stained with Rhodamine 123. To visualize actin, cells were fixed and stained with rhodamine phalloidin and visualized as described by Van Gestel et al. (2002).

Preparation of Microsomal and Plasma Membrane Fractions

Four-day-old NT-1 cells were harvested by filtration and immediately homogenized in 3 volumes of cold buffer as described (Perera et al., 2002), and the crude extract was clarified by centrifugation (5000g for 10 min at 4°C) to yield total cell lysate or fractionated further (40,000g, for 60 min, at 4°C) to yield microsomal and soluble protein fractions. Plasma membrane-enriched fractions were prepared from microsomes by aqueous two-phase partitioning as described previously (Perera et al., 1999). For enzyme assays, membrane fractions were placed on ice and assayed immediately. Protein concentrations were estimated using the Bio-Rad protein assay reagent with BSA as a standard.

Isolation of F-Actin from Plasma Membrane

F-actin was isolated from equal amounts of plasma membrane protein as described previously using a 20,000g centrifugation to recover large actin filaments and bundles (Stevenson-Paulik et al., 2003). After two rounds of polymerization, the 20,000g F-actin pellet was resuspended to a volume equal to the supernatant, and 20 μL of supernatant and pellet were assayed for PtdInsP 5-kinase activity as described below.

Immunoblotting

Immunoblotting was performed by SDS-PAGE of isolated proteins and transferred to a polyvinylidene difluoride membrane by electroblotting. Membranes were blocked with 3% (w/v) BSA, incubated with antibodies (anti-mouse GFP [Clontech] or anti-rabbit BiP and CRT), and incubated with horseradish peroxidase-conjugated anti-mouse or anti-rabbit. Immunoreactivity was visualized by incubating the blot in SuperSignal West Pico Chemiluminescent substrate (Pierce) and exposure to x-ray film. After chemiluminescence detection, total protein was visualized by staining the blots with Amido black (Sigma-Aldrich).

PtdInsP 5-Kinase Assays

In vitro lipid kinase assays were performed using 2 μg of plasma membrane protein. The standard assay was as previously described (Perera et al., 2002) with the following modifications. Reactions were performed either in the absence or presence of substrate [125 μM PtdIns(4)P from porcine brain; Avanti Polar Lipids] at room temperature for 10 min in a total volume of 50 μL . After incubation, phospholipids were extracted and separated by TLC as described (Perera et al., 2002).

Ins(1,4,5)P₃ Assays and PtdIns(4,5)P₂ Mass Measurements

Cells were harvested by filtration and immediately frozen in liquid N_2 , ground to a fine powder, and precipitated with cold 10% (v/v) perchloric acid (PCA). Ins(1,4,5)P₃ assays were performed using the TRK1000 Ins(1,4,5)P₃ assay kit (Amersham Pharmacia Biotech) as previously described (Perera et al., 1999, 2002), and PtdIns(4,5)P₂ mass measurements were performed as described (Heilmann et al., 2001).

Lipid Profiling

To determine the effects of Hs PIPK1 α expression on the plasma membrane lipid profile, we isolated plasma membrane-enriched fractions from 4-d-old wild-type and tobacco cells as described above. Lipid extraction, lipid analysis, and lipid quantification were performed as described (Welti et al., 2002) at the Kansas Lipidomics Facility.

In Vivo Labeling of Cells

In vivo labeling was performed with cells growing at the same rate and that had equivalent fresh weights. For 24-h labeling studies, 5 mL of cultures of 3-d-old wild-type and transgenic cells (~ 0.1 g cells mL^{-1}) were labeled with 25 μCi *myo*-[2-³H] inositol (25 Ci mmol^{-1}). After 24 h, cells were harvested by filtration, ground in liquid N_2 , and incubated with cold 5% (v/v) PCA for 15 min on ice. The pellet and supernatant were separated by centrifugation, the pellet was washed with cold water twice, and the lipids were extracted as described previously (Perera et al., 2002). Extracted lipids were separated by TLC and quantified using a Bioscan imaging scanner or further processed for head group analysis. The phospholipids were deacylated for HPLC analysis as previously described (Hama et al., 2004). For soluble inositol phosphate analysis, cells were labeled as described above for 18 h and precipitated with PCA. The supernatant was analyzed by HPLC for soluble inositol phosphates using a Partisphere SAX strong anion exchange column as described by Stevenson-Paulik et al. (2006).

For short-term labeling, 4-d-old cells were harvested by filtration, weighed, preequilibrated in conditioned medium (0.2 g mL^{-1}), and maintained by shaking. Conditioned medium was pooled from all the cell lines. After a 30-min recovery period, cells were labeled with carrier-free [³²P] Pi (100 $\mu\text{Ci mL}^{-1}$). Equal aliquots (500 μL) of cells were removed at the indicated time points and added immediately to 500 μL of cold 20% (v/v) PCA and incubated on ice for ~ 20 min. The pellet was washed with cold water twice, and lipids were extracted, separated by TLC, and quantified as described above.

O₂ Uptake

Tobacco cells (4 d after transfer) were collected by filtration and pre-equilibrated in fresh medium at 0.1 g fresh weight mL^{-1} for 2 h on a rotary shaker (125 rpm, 25°C). Two-milliliter aliquots were used for measuring the rate of O₂ uptake in a Clarke-type oxygen electrode system from Hansatech Instrument. The O₂ concentration in the solution was measured over time at 25°C and recorded by an Omnitracer recorder (Houston Instruments).

ATPase Activity

Plasma membrane ATPase activity was determined as previously described (Wheeler and Boss, 1987) with and without the addition of V_2O_5 . The vanadate-sensitive ATP hydrolysis is reported.

Calcium Uptake and Release Measurements

Ca^{2+} uptake and release were measured with ER-enriched microsomal membrane fraction as previously described (Persson et al., 2001). Ca^{2+} transport was measured with and without the addition of 3 mM ATP. Ca^{2+} release was determined from [$^{45}Ca^{2+}$]-loaded (23 min) vesicles by adding 1.5 μ M ionomycin ionophore, and membrane vesicles were analyzed for [$^{45}Ca^{2+}$] after 5 min. The net release was determined as difference of [$^{45}Ca^{2+}$] recovered after the addition of ionomycin versus addition of dimethyl sulfoxide (same concentration as in the ionomycin stock) alone.

Whole-Cell Calcium Measurements

Cells (4 and 6 d old) were collected by filtration, washed twice with 5 mL of deionized water, and freeze-dried. The samples were dry ashed at 500°C overnight and digested in 6 N HCl according to Gorsuch (1970), and total calcium was determined using ICP emission spectrometry at the North Carolina State University Analytical Services Laboratory under the direction of Wayne Robarge.

Sugar Analysis

The sugar remaining in the culture medium was measured at the indicated day after transfer using Anthrone reagent as described by Van Handel (1985).

Accession Numbers

Sequence data from this article can be found in the GenBank/EMBL data libraries under accession numbers At4g01190 (*Arabidopsis* PIPK10) and NM_003557 (human PIPK1 α).

Supplemental Data

The following materials are available in the online version of this article.

Supplemental Video 1. A Movie Showing the Localization of GFP-Hs PIPK1 α with the Plasma Membranes of Tobacco Cells in Normal Medium.

Supplemental Video 2. A Movie Showing the Localization of GFP-Hs PIPK1 α with the Plasma Membranes of Tobacco Cells after the Addition of 0.6 Osmolal Sorbitol.

Supplemental Figure 1. Head Group Analysis of PtdIns(4)P and PtdIns(4,5)P₂ from the GFP and Hs PIPK1 α Cell Lines.

Supplemental Figure 2. Calcium Uptake into the Mitochondria and Whole Cells.

Supplemental Figure 3. Ratiometric Imaging of Intracellular Calcium Using the Ca^{2+} Indicator, Indo-1.

Supplemental Figure 4. Visualization of Mitochondria with Rhodamine 123.

Supplemental Figure 5. Visualization of Actin with Rhodamine-Phalloidin.

ACKNOWLEDGMENTS

We thank Richard Anderson (University of Wisconsin) for the gift of the human type I α PIPK, Rebecca S. Boston (North Carolina State Univer-

sity) for the antibodies to CRT and BiP, and Wayne P. Robarge (North Carolina State University) for ICP analysis of calcium. This work was supported in part by funding from the North Carolina Agricultural Research Service (W.F.B. and N.S.A.), the National Science Foundation (W.F.B.), and by the Binational Science Foundation (W.F.B. and Nava Moran). The Kansas Lipidomics Research Center was supported by National Science Foundation Grants MCB0455318 and DBI 0521587, and National Science Foundation EPSCoR Grant EPS-0236913 with matching support from the State of Kansas through Kansas Technology Enterprise Corporation and Kansas State University. The Kansas Lipidomics Research Center is also supported by K-INBRE (National Institutes of Health Grant P20 RR16475 from the INBRE program of the National Center for Research Resources).

Received February 24, 2007; revised April 18, 2007; accepted April 23, 2007; published May 11, 2007.

REFERENCES

- Adel-Latif, A.A., Smith, J.P., and Akhtar, R.A. (1985). Polyphosphoinositides and muscarinic cholinergic and β -adrenergic receptors in iris smooth muscle. In *Inositol and Phosphoinositides: Metabolism and Regulation*, J.E. Bleasdale, J. Eichberg, and G. Hauser, eds (Clifton, NJ: Humana Press), pp. 275–298.
- Akesson, A., Persson, S., Love, J., Boss, W.F., Widell, S., and Sommarin, M. (2005). Overexpression of the Ca^{2+} -binding protein calreticulin in the endoplasmic reticulum improves growth of tobacco cell suspensions (*Nicotiana tabacum*) in high- Ca^{2+} medium. *Plant* **123**: 92–99.
- Berdy, S.E., Kudla, J., Gruissem, W., and Gillasp, G.E. (2001). Molecular characterization of At5PTase1, an inositol phosphatase capable of terminating inositol trisphosphate signaling. *Plant Physiol.* **126**: 801–810.
- Brearley, C.A., and Hanke, D.E. (1996). Metabolic evidence for the order of addition of individual phosphate esters to the myo-inositol moiety of inositol hexakisphosphate in the duckweed *Spirodela polyrhiza* L. *Biochem. J.* **314**: 227–233.
- Burnette, R.N., Gunesekeera, B.M., and Gillasp, G.E. (2003). An *Arabidopsis* inositol 5-phosphatase gain-of-function alters abscisic acid signaling. *Plant Physiol.* **132**: 1011–1019.
- Chen, H., Nelson, R.S., and Sherwood, J.L. (1994). Enhanced recovery of transformants of *Agrobacterium tumefaciens* after freeze-thaw transformation and drug selection. *Biotechniques* **16**: 664–668, 670.
- Cheng, N.-H., Pittman, J.K., Shigaki, T., Lachmansingh, J., LeClere, S., Lahner, B., Salt, D.E., and Hirschi, K.D. (2005). Functional association of *Arabidopsis* CAX1 and CAX3 is required for normal growth and ion homeostasis. *Plant Physiol.* **138**: 2048–2060.
- Cunningham, E., Thomas, G.M., Ball, A., Hiles, I., and Cockcroft, S. (1995). Phosphatidylinositol transfer protein dictates the rate of inositol trisphosphate production by promoting the synthesis of PIP₂. *Curr. Biol.* **5**: 775–783.
- Davis, A.J., Im, Y.J., Dubin, J.S., Tomer, K.B., and Boss, W.F. (2007). *Arabidopsis* phosphatidylinositol phosphate kinase 1 binds F-actin and recruits phosphatidylinositol 4-kinase beta 1 to the actin cytoskeleton. *J. Biol. Chem.* **282**: 14121–14131.
- DeWald, D.B., Torabinejad, J., Jones, C.A., Shope, J.C., Cangelosi, A.R., Thompson, J.E., Prestwich, G.D., and Hama, H. (2001). Rapid accumulation of phosphatidylinositol 4,5-bisphosphate and inositol 1,4,5-trisphosphate correlates with calcium mobilization in salt-stressed *Arabidopsis*. *Plant Physiol.* **126**: 759–769.
- Dowd, P.E., Coursol, S., Skirpan, A.L., Kao, T.H., and Gilroy, S. (2006). Petunia phospholipase C1 is involved in pollen tube growth. *Plant Cell* **18**: 1438–1453.

- Drøbak, B.K., Dewey, R.E., and Boss, W.F.** (1999). Phosphoinositide kinases and the synthesis of polyphosphoinositides in higher plant cells. In *International Review of Cytology*, K.W. Jeon, ed (New York: Academic Press), pp. 95–130.
- Elge, S., Brearley, C., Xia, H.J., Kehr, J., Xue, H.W., and Mueller-Roeber, B.** (2001). An *Arabidopsis* inositol phospholipid kinase strongly expressed in procambial cells: Synthesis of PtdIns(4,5)P₂ and PtdIns(3,4,5)P₃ in insect cells by 5-phosphorylation of precursors. *Plant J.* **26**: 561–571.
- Ercetin, M.E., and Gillaspay, G.E.** (2004). Molecular characterization of an *Arabidopsis* gene encoding a phospholipid-specific inositol polyphosphate 5-phosphatase. *Plant Physiol.* **135**: 938–946.
- Gilroy, S., Read, N.D., and Trewavas, A.J.** (1990). Elevation of cytoplasmic calcium by caged calcium or caged inositol triphosphate initiates stomatal closure. *Nature* **346**: 769–771.
- Gorsuch, T.T.** (1970). *The Destruction of Organic Matter*. (Elmsford, NY: Pergamon Press).
- Gross, W., and Boss, W.F.** (1993). Inositol phospholipids and signal transduction. In *Control of Plant Gene Expression*, D.P.S. Verma, ed (Boca Raton, FL: CRC Press), pp. 17–32.
- Hama, H., Torebinejad, J., Prestwich, G., and DeWald, D.** (2004). Measurement and immunofluorescence of cellular phosphoinositides. In *Methods in Molecular Biology: Signal Transduction Protocols*, R. Dickson, ed (Clifton, NJ: Humana Press), pp. 243–258.
- Haseloff, J., and Amos, B.** (1995). GFP in plants. *Trends Genet.* **11**: 328–329.
- Heilmann, I., Perera, I.Y., Gross, W., and Boss, W.F.** (2001). Plasma membrane phosphatidylinositol 4,5-bisphosphate decreases with time in culture. *Plant Physiol.* **126**: 1507–1518.
- Helling, D., Possart, A., Cottier, S., Klahre, U., and Kost, B.** (2006). Pollen tube tip growth depends on plasma membrane polarization mediated by tobacco PLC3 activity and endocytic membrane recycling. *Plant Cell* **18**: 3519–3534.
- Hunt, L., Mills, L.N., Pical, C., Leckie, C.P., Aitken, F.L., Kopka, J., Mueller-Roeber, B., McAinsh, M.R., Hetherington, A.M., and Gray, J.E.** (2003). Phospholipase C is required for the control of stomatal aperture by ABA. *Plant J.* **34**: 47–55.
- Im, Y.J., Davis, A.J., Perera, I.Y., Johannes, E., Allen, N.S., and Boss, W.F.** (2007). The N-terminal membrane occupation and recognition nexus domain of *Arabidopsis* phosphatidylinositol phosphate kinase 1 regulates enzyme activity. *J. Biol. Chem.* **282**: 5443–5452.
- Kanzaki, M., Furukawa, M., Raab, W., and Pessin, J.E.** (2004). Phosphatidylinositol 4,5-bisphosphate regulates adipocyte actin dynamics and GLUT4 vesicle recycling. *J. Biol. Chem.* **279**: 30622–30633.
- Kunz, J., Fuelling, A., Kolbe, L., and Anderson, R.A.** (2002). Stereospecific substrate recognition by phosphatidylinositol phosphate kinases is swapped by changing a single amino acid residue. *J. Biol. Chem.* **277**: 5611–5619.
- Kunz, J., Wilson, M.P., Kisseleva, M., Hurley, J.H., Majerus, P.W., and Anderson, R.A.** (2000). The activation loop of phosphatidylinositol phosphate kinases determines signaling specificity. *Mol. Cell* **5**: 1–11.
- Lievremont, J.P., Rizzuto, R., Hendershot, L., and Meldolesi, J.** (1997). BiP, a major chaperone protein of the endoplasmic reticulum lumen, plays a direct and important role in the storage of the rapidly exchanging pool of Ca²⁺. *J. Biol. Chem.* **272**: 30873–30879.
- Logan, D.C., and Knight, M.R.** (2003). Mitochondrial and cytosolic calcium dynamics are differentially regulated in plants. *Plant Physiol.* **133**: 21–24.
- Lou, Y., Gou, J.-Y., and Xue, H.-W.** (2007). PIP5K9, an *Arabidopsis* phosphatidylinositol monophosphate kinase, interacts with a cytosolic invertase to negatively regulate sugar-mediated root growth. *Plant Cell* **19**: 163–181.
- McCormack, J.G., and Denton, R.M.** (1993). Mitochondrial Ca²⁺ transport and the role of intramitochondrial Ca²⁺ in the regulation of energy metabolism. *Dev. Neurosci.* **15**: 165–173.
- McCormack, J.G., Halestrap, A.P., and Denton, R.M.** (1990). Role of calcium ions in regulation of mammalian intramitochondrial metabolism. *Physiol. Rev.* **70**: 391–425.
- Meijer, H.J.G., and Munnik, T.** (2003). Phospholipid-based signaling in plants. *Annu. Rev. Plant Biol.* **54**: 265–306.
- Michalak, M., Corbet, E.F., Mesaeli, N., Nakamura, K., and Opas, M.** (1999). Calreticulin: One protein, one gene, many functions. *Biochem. J.* **344**: 281–292.
- Mikami, K., Katagiri, T., Iuchi, S., Yamaguchi-Shinozaki, K., and Shinozaki, K.** (1998). A gene encoding phosphatidylinositol-4-phosphate 5-kinase is induced by water stress and abscisic acid in *Arabidopsis thaliana*. *Plant J.* **15**: 563–568.
- Mueller-Roeber, B., and Pical, C.** (2002). Inositol phospholipid metabolism in *Arabidopsis*. Characterized and putative isoforms of inositol phospholipid kinase and phosphoinositide-specific phospholipase C. *Plant Physiol.* **130**: 22–46.
- Munnik, T., Irvine, R.F., and Musgrave, A.** (1998). Phospholipid signalling in plants. *Biochim. Biophys. Acta* **1389**: 222–272.
- Pappan, K., and Wang, X.** (1999). Plant phospholipase D α is an acidic phospholipase active at near-physiological Ca²⁺ concentrations. *Arch. Biochem. Biophys.* **368**: 347–353.
- Perera, I.Y., Davis, A.J., Galanopoulou, D., Im, Y.J., and Boss, W.F.** (2005). Characterization and comparative analysis of *Arabidopsis* phosphatidylinositol phosphate 5-kinase 10 reveals differences in *Arabidopsis* and human phosphatidylinositol phosphate kinases. *FEBS Lett.* **579**: 3427–3432.
- Perera, I.Y., Heilmann, I., and Boss, W.F.** (1999). Transient and sustained increases in inositol 1,4,5-trisphosphate precede the differential growth response in gravistimulated maize pulvini. *Proc. Natl. Acad. Sci. USA* **96**: 5838–5843.
- Perera, I.Y., Hung, C.Y., Brady, S., Muday, G.K., and Boss, W.F.** (2006). A universal role for inositol 1,4,5-trisphosphate-mediated signaling in plant gravitropism. *Plant Physiol.* **140**: 746–760.
- Perera, I.Y., Love, J., Heilmann, I., Thompson, W.F., and Boss, W.F.** (2002). Up-regulation of phosphoinositide metabolism in tobacco cells constitutively expressing the human type I inositol polyphosphate 5-phosphatase. *Plant Physiol.* **129**: 1795–1806.
- Persson, S., Love, J., Tsou, P.-L., Robertson, D., Thompson, W.F., and Boss, W.F.** (2002). When a day makes a difference. Interpreting data from endoplasmic reticulum-targeted green fluorescent protein fusions in cells grown in suspension culture. *Plant Physiol.* **128**: 341–344.
- Persson, S., Wyatt, S.E., Love, J., Thompson, W.F., Robertson, D., and Boss, W.F.** (2001). The Ca²⁺ status of the endoplasmic reticulum is altered by induction of calreticulin expression in transgenic plants. *Plant Physiol.* **126**: 1092–1104.
- Phillippy, B.Q.** (1998). Identification of inositol 1,3,4-trisphosphate 5-kinase and inositol 1,3,4,5-tetrakisphosphate 6-kinase in immature soybean seeds. *Plant Physiol.* **116**: 291–297.
- Pical, C., Westergren, T., Dove, S.K., Larsson, C., and Sommarin, M.** (1999). Salinity and hyperosmotic stress induce rapid increases in phosphatidylinositol 4,5-bisphosphate, diacylglycerol pyrophosphate, and phosphatidylcholine in *Arabidopsis thaliana* cells. *J. Biol. Chem.* **274**: 38232–38240.
- Poggioli, J., Weiss, S.J., McKinney, J.S., and Putney, J.W., Jr.** (1983). Effects of antimycin A on receptor-activated calcium mobilization and phosphoinositide metabolism in rat parotid gland. *Mol. Pharmacol.* **23**: 71–77.
- Preuss, M.L., Schmitz, A.J., Thole, J.M., Bonner, H.K., Otegui, M.S., and Nielsen, E.** (2006). A role for the RabA4b effector protein PI-4Kbeta1 in polarized expansion of root hair cells in *Arabidopsis thaliana*. *J. Cell Biol.* **172**: 991–998.
- Raboy, V.** (2001). Seeds for a better future: 'Low phytate' grains help to overcome malnutrition and reduce pollution. *Trends Plant Sci.* **6**: 458–462.

- Ridley, A.J. (2006). Rho GTPases and actin dynamics in membrane protrusions and vesicle trafficking. *Trends Cell Biol.* **16**: 522–529.
- Rozelle, A.L., Machesky, L.M., Yamamoto, M., Driessens, M.H., Insall, R.H., Roth, M.G., Luby-Phelps, K., Marriott, G., Hall, A., and Yin, H.L. (2000). Phosphatidylinositol 4,5-bisphosphate induces actin-based movement of raft-enriched vesicles through WASP-Arp2/3. *Curr. Biol.* **10**: 311–320.
- Sandelius, A.S., and Sommarin, M. (1990). Membrane-localized reactions involved in polyphosphoinositide turnover in plants. In *Inositol Metabolism in Plants*, D.J. Morre, W.F. Boss, and F.A. Loewus, eds (New York: Wiley-Liss), pp. 139–161.
- Stevenson-Paulik, J., Chiou, S.T., Frederick, J.P., Cruz, J.D., Seeds, A.M., Otto, J.C., and York, J.D. (2006). Inositol phosphate metabolomics: Merging genetic perturbation with modernized radiolabeling methods. *Methods* **39**: 112–121.
- Stevenson-Paulik, J., Love, J., and Boss, W.F. (2003). Differential regulation of two *Arabidopsis* type III phosphatidylinositol 4-kinase isoforms. A regulatory role for the pleckstrin homology domain. *Plant Physiol.* **132**: 1053–1064.
- Stevenson-Paulik, J., Odom, A.R., and York, J.D. (2002). Molecular and biochemical characterization of two plant inositol polyphosphate 6-/3-/5-kinases. *J. Biol. Chem.* **277**: 42711–42718.
- Stevenson, J.M., Perera, I.Y., and Boss, W.F. (1998). A phosphatidylinositol 4-kinase pleckstrin homology domain that binds phosphatidylinositol 4-monophosphate. *J. Biol. Chem.* **273**: 22761–22767.
- Stevenson, J.M., Perera, I.Y., Heilmann, I., Persson, S., and Boss, W.F. (2000). Inositol signaling and plant growth. *Trends Plant Sci.* **5**: 252–258.
- Subbaiah, C.C., Bush, D.S., and Sachs, M.M. (1998). Mitochondrial contribution to the anoxic Ca^{2+} signal in maize suspension-cultured cells. *Plant Physiol.* **118**: 759–771.
- Tan, Z., and Boss, W.F. (1992). Association of phosphatidylinositol kinase, phosphatidylinositol monophosphate kinase, and diacylglycerol kinase with the cytoskeleton and F-actin fractions of carrot (*Daucus carota* L.) cells grown in suspension culture. *Plant Physiol.* **100**: 2116–2120.
- Tucker, E.B., and Boss, W.F. (1996). Mastoparan-induced intracellular Ca^{2+} fluxes may regulate cell-to-cell communication in plants. *Plant Physiol.* **111**: 459–467.
- Van Gestel, K., Kohler, R.H., and Verbelen, J.P. (2002). Plant mitochondria move on F-actin, but their positioning in the cortical cytoplasm depends on both F-actin and microtubules. *J. Exp. Bot.* **53**: 659–667.
- Van Handel, E. (1985). Rapid determination of glycogen and sugars in mosquitoes. *J. Am. Mosq. Control Assoc.* **1**: 299–301.
- Van Leeuwen, W., Okresz, L., Bogre, L., and Munnik, T. (2004). Learning the lipid language of plant signalling. *Trends Plant Sci.* **9**: 378–384.
- Verma, D.P.S., and MacLachlan, G.A. (1976). Metabolism of poly(A) in plant cells: Discrete classes associated with free and membrane-bound polysomes. *Plant Physiol.* **58**: 405–410.
- Vincent, P., Chua, M., Nogue, F., Fairbrother, A., Mekeel, H., Xu, Y., Allen, N., Bibikova, T.N., Gilroy, S., and Bankaitis, V.A. (2005). A Sec14p-nodulin domain phosphatidylinositol transfer protein polarizes membrane growth of *Arabidopsis thaliana* root hairs. *J. Cell Biol.* **168**: 801–812.
- Wang, C., and Wang, X. (2001). A novel phospholipase D of *Arabidopsis* that is activated by oleic acid and associated with the plasma membrane. *Plant Physiol.* **127**: 1102–1112.
- Wang, X. (2000). Multiple forms of phospholipase D in plants: The gene family, catalytic and regulatory properties, and cellular functions. *Prog. Lipid Res.* **39**: 109–149.
- Welti, R., Li, W., Li, M., Sang, Y., Biesiada, H., Zhou, H.-E., Rajashekar, C.B., Williams, T.D., and Wang, X. (2002). Profiling membrane lipids in plant stress responses. Role of phospholipase $D\alpha$ in freezing-induced lipid changes in *Arabidopsis*. *J. Biol. Chem.* **277**: 31994–32002.
- Westergren, T., Dove, S.K., Sommarin, M., and Pical, C. (2001). AtPIP5K1, an *Arabidopsis thaliana* phosphatidylinositol phosphate kinase, synthesizes PtdIns(3,4)P₂ and PtdIns(4,5)P₂ in vitro and is inhibited by phosphorylation. *Biochem. J.* **359**: 583–589.
- Westergren, T., Ekblad, L., Jergil, B., and Sommarin, M. (1999). Phosphatidylinositol 4-kinase associated with spinach plasma membranes. Isolation and characterization of two distinct forms. *Plant Physiol.* **121**: 507–516.
- Wheeler, J.J., and Boss, W.F. (1987). Polyphosphoinositides are present in plasma membranes isolated from fusogenic carrot cells. *Plant Physiol.* **85**: 389–392.
- Williams, M.E., Torabinejad, J., Cohick, E., Parker, K., Drake, E.J., Thompson, J.E., Hortter, M., and Dewald, D.B. (2005). Mutations in the *Arabidopsis* phosphoinositide phosphatase gene SAC9 lead to overaccumulation of PtdIns(4,5)P₂ and constitutive expression of the stress-response pathway. *Plant Physiol.* **138**: 686–700.
- Wu, Z., Liang, F., Hong, B., Young, J.C., Sussman, M.R., Harper, J.F., and Sze, H. (2002). An endoplasmic reticulum-bound Ca^{2+} /Mn²⁺ pump, ECA1, supports plant growth and confers tolerance to Mn²⁺ stress. *Plant Physiol.* **130**: 128–137.
- Yamamoto, K., and Kiss, J.Z. (2002). Disruption of the actin cytoskeleton results in the promotion of gravitropism in inflorescence stems and hypocotyls of *Arabidopsis*. *Plant Physiol.* **128**: 669–681.
- Yeung, T., Terebiznik, M., Yu, L., Silvius, J., Abidi, W.M., Phillips, M., Levine, T., Kapus, A., and Grinstein, S. (2006). Receptor activation alters inner surface potential during phagocytosis. *Science* **313**: 347–351.
- Zhong, R., Burk, D.H., Morrison III, W.H., and Ye, Z.H. (2004). FRAGILE FIBER3, an *Arabidopsis* gene encoding a type II inositol polyphosphate 5-phosphatase, is required for secondary wall synthesis and actin organization in fiber cells. *Plant Cell* **16**: 3242–3259.